



Published in final edited form as:

*Neurol Res.* 2019 March ; 41(3): 257–264. doi:10.1080/01616412.2018.1554284.

## Diffusion Tensor Tractography to Visualize Axonal Outgrowth and Regeneration in a 4-cm Reverse Autograft Sciatic Nerve Rabbit Injury Model

Angel F. Farinas, MD<sup>1</sup>, Alonda C. Pollins, MLI<sup>1</sup>, Michael Stephanides, BA<sup>6</sup>, Dillon O'Neill, MD<sup>7</sup>, Salam Al-Kassis, MD<sup>1</sup>, Isaac V. Manzanera Esteve, PhD<sup>3,4</sup>, Juan M. Colazo, BS<sup>5</sup>, Patrick R. Keller, BS<sup>5</sup>, Timothy Rankin, MD<sup>1</sup>, Blair A. Wormer, MD<sup>1</sup>, Christodoulos Kaoutzanis, MD<sup>1</sup>, Richard D. Dortch, PhD<sup>2,3,4</sup>, and Wesley P. Thayer, MD, PhD<sup>1,2</sup>

<sup>1</sup>Vanderbilt University Medical Center, Department of Plastic Surgery, Nashville, TN

<sup>2</sup>Vanderbilt University, Department of Biomedical Engineering, Nashville, TN

<sup>3</sup>Vanderbilt University Medical Center, Department Radiology and Radiological Sciences, Nashville, TN

<sup>4</sup>Vanderbilt University Medical Center, Institute of Imaging Science, Nashville, TN

<sup>5</sup>Vanderbilt University School of Medicine, Nashville, TN

<sup>6</sup>Meharry School of Medicine, Nashville, TN

<sup>7</sup>University of Utah, Department of Orthopedics, Salt Lake City, UT

### Abstract

**Background:** Diffusion tensor tractography (DTT) has recently been shown to accurately detect nerve injury and regeneration. This study assesses whether 7-tesla (7T) DTT imaging is a viable modality to observe axonal outgrowth in a 4 cm rabbit sciatic nerve injury model fixed by a reverse autograft surgical technique.

**Methods:** Transection injury of unilateral sciatic nerve (4 cm long) was performed in 25 rabbits and repaired using a reverse autograft (RA) surgical technique. Analysis of the nerve autograft was performed at 3, 6, and 11 weeks postoperatively and compared to normal contralateral sciatic nerve, used as control group. High-resolution DTT from *ex vivo* sciatic nerves were obtained using 3D diffusion-weighted spin-echo acquisitions at 7-T. Total axons and motor and sensory axons were counted at defined lengths along the graft.

**Results:** At 11 weeks, histologically, the total axon count of the RA group was equivalent to the contralateral uninjured nerve control group. Similarly, by qualitative DTT visualization, the 11-week RA group showed increased fiber tracts compared to the 3 and 6 weeks counterparts. Upon immunohistochemical evaluation, 11-week motor axon counts did not significantly differ between

---

**Corresponding author:** Wesley P. Thayer, Department of Plastic Surgery, Vanderbilt University Medical Center, 1161 21st Ave S, MCN D4207, Nashville, TN 37232-2345, Phone: 615-936-3759, Fax: 615-936-0167, wesley.thayer@vumc.org.

**Disclosures:** The authors declare that they have no conflict of interest

reverse autograft and control; but significantly decreased sensory axon counts remained. Nerves explanted at 3 weeks and 6 weeks showed decreased motor and sensory axon counts.

**Discussion:** 7-T DTT is an effective imaging modality that may be used qualitatively to visualize axonal outgrowth and regeneration. This has implications for the development of technology that non-invasively monitors peripheral nerve regeneration in a variety of clinical settings.

### Keywords

Reverse autograft; diffusion tensor tractography; MRI; peripheral nerve regeneration; sciatic nerve injury

---

### Introduction

Peripheral nerve injuries can create devastating long-term functional deficits. Car accidents, gunshot wounds, deep cuts, oncological resection, and other traumas can cause significant peripheral nerve damage leading to loss of function in limbs with little chance for recovery. Developing effective and efficient repair techniques for nerve injury is important for both our civilian population and our military population. Recent advancements in body armor and emergency medical procedures have dramatically increased the number of wounded soldiers and civilians who survive with severe wounds to the limbs.<sup>1</sup> A study by Stansbury et al. (2008) demonstrated that extremity injuries made up 54% of all combat wounds sustained in Operation Iraqi Freedom and Operation Enduring Freedom.<sup>2</sup> One of the most debilitating and mentally challenging outcomes for these patients is amputation. One of the key determinants for amputation is concomitant nerve injury with dismal hope for recovery.<sup>2</sup> Due to nerve injuries' significant contribution to poor clinical outcomes, there is compelling rationale to improve nerve repair techniques and as well as the ways in which we monitor nerve recovery over time.

The peripheral nervous system, unlike the central nervous system, has a remarkable resilience to injury because of its ability to regenerate axons.<sup>3</sup> Axons in peripheral nerves can grow distally at a rate of about 1 mm per day.<sup>4</sup> This recovery, however, requires a complex interaction between cells, growth factors, and the extracellular matrix.<sup>5</sup> After being transected, proximal segments form growth cones that respond to neurotrophic and chemotropic signals to direct neurite outgrowth.<sup>3</sup> Fibroblasts and Schwann cells produce growth factors that promote neuron survival or cell death.<sup>6</sup> Extracellular matrix can stimulate or inhibit growth of the nerve and serve as a guiding substrate for nerve regeneration.<sup>6</sup> This ability for the nerve to recover, however, may not lead to a functional recovery in the limb. Chronic denervation may cause the muscle atrophy by the time the nerve is able to reinnervate the target tissue.<sup>7</sup> Recovering axons may behave in an unpredictable manner as well. Abnormal axonal regrowth and neuroma formation, physical barriers to innervation, and anterograde degeneration severely complicate recovery.<sup>6</sup>

A plethora of techniques are in use or are currently being developed to improve recovery of nerves.<sup>8</sup> Novel techniques include hydrophilic polymers such as polyethylene glycol (PEG)<sup>9,10</sup> autogenous vein grafts,<sup>11</sup> and tubes (conduits) made of multiple materials including

collagen, silicone, polyglactin, and polyglycolic acid (PGA).<sup>12</sup>The current gold standard for nerve repair continues to be the autograft, with some studies showing better regeneration if the autograft is reversed in polarity, officially termed “reverse autograft (RA).<sup>13</sup>

Measurement of muscle recruitment with electrodiagnostic testing is the current standard of reference for assessing motor recovery following peripheral nerve injury. However, it is operator-dependent and mildly invasive, requiring needle placement into muscles. To quantify axonal outgrowth in the research setting, the current standard is histological staining, however, this technique requires considerable time, expense, and skill to visualize.<sup>14</sup> Therefore, new techniques are needed for monitoring regeneration of nerves. Preferably non-invasive techniques that can be performed with little to no discomfort to the subject.

Diffusion tensor tractography (DTT) is a magnetic resonance imaging (MRI) technique that enables the visualization of nerve degeneration and regeneration.<sup>15</sup> DTT is based upon diffusion tensor imaging (DTI) and yields three-dimensional fiber tracts that represent the orientation of nerve fibers within tissue.<sup>16</sup> Recent studies have demonstrated the accuracy of DTI when compared to functional and histologic outcome parameters when assessing nerve regeneration in animal models.<sup>17</sup> Unfortunately, most of these studies have used small animal models with small nerve transections; which has little translatability to human peripheral nerve injuries.<sup>18</sup>

The objective of this study was to evaluate the qualitative DTT technique as a viable imaging technique for observing axonal outgrowth in large (4 cm) nerve deficit repairs, when using the gold standard reverse autograft technique against standard histological methods of assessment.

## Methods

### Animal Model

New Zealand White rabbits were purchased from a USDA certified vendor utilized by Vanderbilt University Medical Center. All procedures were reviewed and approved under the number M1600136–00, by Institutional Animal Care and Use Committee (IACUC); in accordance to the Guide for Care and Use of Laboratory Animals to minimize suffering and pain. Twenty-nine rabbits were utilized for this study. The average preoperative weight of the rabbits was 3.2 kg.

### Operative Technique

Rabbits were given a mixture of Ketamine (40 mg/kg) and Xylazine (9 mg/kg) intramuscularly to induce anesthesia. Anesthesia was maintained under general endotracheal anesthesia with Isoflurane 2% at 3 ml/min. Rabbits were prepped and draped in sterile fashion. A 5-cm incision was performed longitudinally parallel to the femur. Using a combination of blunt and sharp dissection, the sciatic nerve was exposed in a muscle sparing approach. Sciatic nerves were sharply transected twice, resulting in a 40mm deficit and a 40mm graft, which was then reversed 180 degrees and then sutured back in place of the deficit. The epineurial layer was secured using 9–0 nylon suture (Ethicon, Somerville, NJ). The muscle plane was closed by layers using a 3–0 vicryl (Ethicon, Somerville, NJ) in an

interrupted horizontal mattress fashion and cutaneous closure was achieved with 5–0 monocryl (Ethicon, Somerville, NJ) in a running subcuticular fashion.

### Postoperative Care

Rabbits were observed until they recovered from anesthesia before being transported back to our institution's rabbit room in accordance with approved protocols. For pain control, rabbits received 24 hours of postoperative buprenorphine hydrochloride (Bupranex) dosed every 8 hours. In addition, rabbits received 72 hours of meloxicam dosed every 24 hours.

Rabbits were housed individually in Allentown rabbit cage rack systems. Non-contact (Techboard) was placed in plastic pans underneath the racks to collect feces and urine. Cages were changed biweekly. The rabbits were fed one cup of High Fiber Lab Rabbit Diet (Lab Supply, Fort Worth, TX). All food was replaced daily. Rabbits had free access to food and water 24 hours a day through automatic feeders. Automatic light timers were set for 12-hour cycles with light on between 6:00 am and 6:00 pm.

Rabbits were weighed weekly and grossly inspected for complications at that time. In addition, animals were observed daily for the development of complications by either study investigators or by animal care staff. At the outset of the protocol, no prophylactic measures were instituted to prevent postoperative complications. At specified postoperative times of 3 weeks, 6 weeks, and 11 weeks the rabbits were euthanized using sodium pentobarbital overdose injected intravenously (125 mg/kg). Nerves were harvested for either immunohistochemistry (IHC) or DTT analysis followed by plastic embedding and total axon counting.

### Exclusion Criteria

Some rabbits were unfortunately euthanized early due to complications. Rabbits were euthanized early in the study if they met any of the following criteria: Self-mutilation of hindlimb with bone exposure, surgical site infection, ulceration of the injured foot with full thickness tissue loss, refusal to eat or drink, 20% weight loss, or immobility reluctant to analgesia. Due to these complications, only 19 rabbits were able to complete the study within the intended time points.

### Histology

Explanted nerve tissue samples intended for immunohistochemistry were divided into sections: proximal to the graft, proximal inside the graft, distal inside the graft, and distal outside the graft. "Proximal" was defined as 5 mm proximal to the proximal repair site, "proximal graft" was 5 mm distal to the proximal repair site, "distal graft" was 5 mm proximal to the distal repair site, and distal was 5 mm distal to the distal repair site. Remaining pieces of these dissected nerves were processed for plastic embedding and total axon counting. Groups for total axon counting included Proximal (3mm proximal to the proximal repair site), graft (in the graft midway between the 2 repair sites), and distal (3mm distal to the distal repair site).

**Immunohistochemistry**—Tissues as previously described, were grossly dissected and fixed in neutral buffered formalin overnight and then processed for paraffin embedding. Tissues were embedded for cross-sectioning in paraffin. Formalin-fixed paraffin embedded tissues were sectioned at 5 $\mu$ m, placed on slides and warmed overnight at 60°C. Immunohistochemical staining was performed using commercial antibodies specifically directed against Carbonic Anhydrase II (CA2) (R&D Systems, Minneapolis, MN) and Choline Acetyltransferase (Millipore, Temecula, CA).

Slides were deparaffinized and rehydrated with graded alcohols ending in Tris buffered saline (TBS-T Wash Buffer, LabVision, Fremont, CA). For CA2, heat mediated target retrieval was performed in 1X Target Retrieval Buffer (DAKO, Carpinteria, CA). Endogenous peroxidases were blocked by incubation in 3% H<sub>2</sub>O<sub>2</sub> (Fisher, Suwanee, GA) in TBS-T. Non-specific background, secondary, and tertiary labeling of target was accomplished by use of Vector's ABC Elite Sheep IgG kit (Vector Laboratories, Burlingame, CA). Primary antibody to CA2 was used at 1:800 for 1 hour. For Choline Acetyltransferase staining, heat mediated target retrieval and peroxidase blocking was performed as before. Non-specific background, secondary, and tertiary labeling of target was accomplished by use of Vector's ABC Elite Goat IgG kit (Vector Laboratories). Primary antibody to Choline Acetyltransferase was used at 1:400 for 1 hour. Slides were rinsed with TBS-T between each reagent treatment and all steps were carried out at room temperature. Visualization was achieved with DAB+ chromogen (DAKO). Slides were counterstained with Mayer's hematoxylin, dehydrated through a series of alcohols and xylenes, and then coverslipped with Acrytol Mounting Media (Surgipath, Richmond, IL).

Digital images of slides were acquired with an Olympus C-35AD-4 microscope. Individual images covering the entire axonal region were taken at 20X. ImageJ was used to measure total immuno-positive axons. Measurements for all individual images of a sample were summed to determine total number of immuno-positive axons within each cross section.

**Toluidine Blue Stain**—Once harvested nerves had been scanned for MRI, they were grossly dissected and processed for plastic embedding. Additional samples for plastic embedding were collected from the remains of the dissected nerves used for immunohistochemistry, as described above. Areas analyzed include proximal, graft, and distal. All graft samples for plastic embedding were taken from the center of the graft. Samples were fixed or post-fixed (if used for MRI) in 2% paraformaldehyde/3% glutaraldehyde, counterstained with 1% OsO<sub>4</sub> solution, dehydrated in increasing concentrations of ethanol, and then embedded in resin at 60° for 72 hours. Samples were sectioned at 1 $\mu$ m and stained with 1% toluidine blue.

Digital images of slides were acquired with an Olympus C-35AD-4 microscope. Total axon area was measured using Image-Pro Plus 7.0. Axon density (axons /  $\mu$ m<sup>2</sup>) was calculated by manually counting axons within 3 randomly selected areas at 40x magnification, then averaged to avoid selection bias. Total axon count was calculated by multiplying the average axon density by the total axon area.

**Statistical Analysis and Graphing**—All statistical analyses were performed using Microsoft Excel. Graphs represent mean values for each treatment group along the length of the repair. Error bars indicate Standard Error of the Mean. Excel's Data Analysis ToolPak was used to perform individual student t tests between test groups. Significance was set at  $p < 0.05$ .

**Preparation of samples for DTT**—Harvested nerves were incubated in 4% glutaraldehyde/0.5% paraformaldehyde in phosphate-buffered saline at 4°C. After 24 hours postfixation, excised nerves were placed in phosphate-buffered saline+2mM Gd-DTPA (Magnevist, Bayer HealthCare, Wayne, NJ) at 4°C for at least 24 hours before imaging. For imaging, excised nerves were placed in 2-mm outer diameter glass capillary tubes filled with a perfluoropolyether liquid (Fomblin, Solvay Solexis, Thorofare, NJ) for susceptibility matching, preventing tissue dehydration, and a signal-free background. For higher throughput, 6 excised sciatic nerves in a hexagonal arrangement were imaged simultaneously.

**Imaging Acquisition**—Data was acquired in a 7-T, 16cm bore Bruker Biospec console (Rheinstetten, Germany) using a 25-mm quadrature Doty Scientific for transmission and reception. High-resolution scans were performed using a TE/TR of 22/425ms, FOV of  $72 \times 72 \times 64 \text{mm}^3$ , for a nominal resolution of  $250 \times 250 \times 500 \mu\text{m}^3$ . DTI was performed using a 3D diffusion-weighted spin-echo sequence, with a  $\delta$  of 4/12 msec, 2 averages, 12 directions with b of  $2000 \text{s/mm}^2$  (and one b of 0 image), and a scan time of 10 hours and 36 minutes.

**Imaging Analysis**—Image data reconstruction was performed using in-house written code in MATLAB (MathWorks, Natick, Mass). DTT analysis was implemented in ExploreDTI toolbox<sup>19</sup> with fractional anisotropy thresholds of 0.25–0.37 and an angular deviation threshold of 30 degrees.

## Results:

### DTT Imaging

Qualitative visual inspection revealed continuous tracts throughout the body of each normal control nerve (Fig. 1A), whereas there were multiple discontinuities present in RA repaired nerves particularly in the 6-week samples (Fig. 1B). Fewer tracts were visible in the proximal segments of injured nerves, most likely due to reduced anisotropy from tissue edema. Additionally, the number of continuous tracts seeded proximally and passing through the injury site and distal were significantly lower in RA repaired nerves. At 11 weeks post op, the RA repaired nerves show similar tractography as the normal controls, except for a slight decrease in distal axonal outgrowth length and width. (Fig. 1C),

### Histology

**Toluidine Blue - Total Axon Counts**—Total axons counts were made from toluidine blue stained cross-sections from 3 locations: proximally to the graft, within the graft, mid-way between the proximal and distal repair sites, and distally from the graft. (Figure 2) All

three reverse autograft time points averaged greater total axons in the proximal region when compared to uninjured control, however this did not prove to be significant. Inside the graft, total axons of the 3-week RA group were significantly less as compared to all other groups. In addition, total axons in the 6-week RA groups within the graft were less than control ( $p=0.013$ ). By 11-weeks, the total axon count in this region was no different than normal control (uninjured contralateral nerve). Similarly, to the measurements within in the graft, the 11-week RA groups was not different from control, while both 3 and 6-week were. Also, 3 and 6-week RA groups were indistinguishable from one another. .

### Immunohistochemistry

**Motor Axon Counts**—In the 3-week RA group, motor axons measurements proximal to the RA did not differ from normal controls. (Figure 3A) As we look along the length of the repair, the motor axon counts decrease. In the 11-week RA group, motor axons, proximal to the repair site, were significantly increased compared to control. For all other sampled locations, there was no difference between 11-week RA and control.

**Sensory Axon Counts**—Sensory axon counts in the 3-week RA group were significantly decreased compared to control at all portions along the nerve ( $p<0.05$ ) . (Figure 3B) This trend was also seen in the 11-week RA groups, however was not statistically significant.

### Discussion:

Prior studies evaluating DTT of peripheral nerve injuries have focused on the effects of crush or contusion with blunt force trauma.<sup>20</sup> Although nerve crush is a significant cause of morbidity, traumatic nerve injuries often involve partial or complete neurotmesis that can result in lifelong disability if not promptly diagnosed and microscopically repaired.<sup>21</sup> Providing a new method of detecting nerve transection could prevent delays in surgical repair that lead to irreversible weakness, loss of function, and other undesirable sequelae. Additionally, DTT could be highly valuable as a tool for assessing nerve repairs and suggesting when a revision surgery is necessary. In the current study, we examined the use of DTT in a 4-cm nerve segmental loss rabbit model that was designed to resemble traumatic nerve injuries seen in humans.

In this study, we demonstrate that DTT of nerve fibers visually correlates with recovery of the population of motor neurons demonstrated with immunohistochemistry. This can be explained by the loss of fiber coherence along degenerated axons, and a subsequent recovery of coherence during the regeneration process.

Time of recovery, as a function of length of nerve transection, is an important clinical variable for both the patient and the surgeon. From a surgeon's perspective, knowing key time points of recovery for certain nerve injuries will allow them to track progress and perform a revision surgery in a timely manner if required. From a patient's perspective, getting back to full function as earliest as possible is always a priority. Many researchers and clinicians claim the "1 mm/day" rule for peripheral nerve regeneration.<sup>4</sup> Peripheral nerve outgrowth was measured using traditional histological methods and correlated with 7-T DTT



findings. Both methods show equal ability to measure outgrowth, but DTT provides the ability to visualize regeneration.

Surgeons and clinicians hope that sensory axons and motor axons can regenerate and repair at the same rate to decrease differences in functional outcomes. Over the years there has been an increasing amount of literature published over preferential motor reinnervation (PMR). PMR refers to the proven ability of regenerating motor axons to preferentially, but still incompletely, reinnervate muscle versus cutaneous distal nerve branches. Previous work with femoral rat nerves has revealed that given equal access, regenerating motor axons preferentially reinnervate the terminal muscle branch.<sup>22,23</sup> Regenerating motor axons initially grow into both nerve branches but over time are pruned from the cutaneous branch.<sup>24</sup> Similarly, in the current study, through histological analysis we observed that motor axons had a higher count number than sensory axons in the harvested nerves 11 weeks post-op.

Clinically, motor nerves will recover in a timelier fashion is important for two main reasons. Firstly, this has led to clinicians preferentially using motor nerve grafts during nerve autograft procedures. A study by Nichols et al. looked at how Lewis rats' sensory vs motor nerve grafts affected the regeneration of a cut mixed nerve system (both motor and sensory nerves). After 3 weeks, a mixed nerve defect had undergone substantial regeneration when paired with a motor nerve graft or a mixed nerve graft. In comparison, the sensory nerve graft was statistically less effective in regeneration, looking specifically at nerve fiber count, percent nerve, and nerve densities.<sup>25</sup> Secondly, being able to move your limbs without pain and sensory feedback can lead to re-injury and overall decreased functional outcomes, especially after a traumatic event in which muscular and other soft-tissue injuries may exist.

There are multiple limitations in this study. Most importantly, this study was conducted on excised sciatic nerves that had been cleaned and cross-linked in fixative prior to imaging. Fixation is known to reduce isotropic diffusion but should have minimal effect on relative tissue anisotropy.<sup>26</sup> A second limitation of this study was the time required for high-resolution image acquisition. For efficient clinical translational of this technology, it will be critical to find the resolution and field of view (FOV) that minimize scan time while maintaining signal-to-noise ratio (SNR) and diagnostic accuracy. A third limitation of this study is that only twenty-five rabbits were able to complete the study due to postoperative complications. The most common postoperative complication with the rabbits was autophagia. Twenty rabbits attempted some form of autophagia leading to compassionate euthanasia. Other areas included between the phalanges, the dorsal aspect of the foot, and the incision site. The second most common postoperative complication was the development of pressure ulcers. Sixteen rabbits developed pressure ulcers. The pressure ulcers appeared on the plantar aspect of the injured foot, near the heel. These generally began as erythematous, alopecic areas on the heel which developed into an eschar. Over time these converted into full thickness defects exposing the underlying tissue and bone. The rate of conversion of these ulcers postoperatively varied. We developed an intervention and were able to salvage nine of these subjects, the rest also qualified for early euthanasia. Other minor complications that did not lead to euthanasia but required extra effort for treatment also occurred. These unfortunate situations precluded us to use behavioral tests performed weekly to validate DTT and histological findings. The location of these complications was



in the affected hind limbs; and thus, clinical evaluations were hindered due to treatment interventions and did not reflect an accurate panorama of recovery.

## Conclusion:

Overall, our results show that regeneration of large (4 cm) gaps can be successfully performed using a reverse autograft technique and that regeneration back to baseline is time-dependent. We found that complete recovery takes longer than 6 weeks with 11 weeks being a predictive timeline marker based on our timepoints. By comparing imaging results to histological analysis, 7-T diffusion tensor imaging looks like a promising qualitative method to analyze anatomical peripheral nerve axonal outgrowth and regeneration. Future work is warranted in studying the preferential growth of motor axons over sensory axons in this model. Additionally, future work in understanding the molecular mechanisms regarding time-dependence of nerve regeneration could lead to new therapeutics capable of increasing postoperative functional outcomes. Lastly, the goal of DTT is for its translation from bench-to bedside allowing for in-vivo imaging of peripheral nerve injuries occurring in human patients. Although recent studies have shown progress towards this goal, it is still very much experimental and further work needs to be done in increasing resolution (image through edema, hematomas, anatomical variations, etc.), speed (reduce patient morbidity and healthcare time/costs), and data quantification (being able to standardize results across different patient populations, times, injuries etc.)

## Acknowledgments

Financial Disclosures Statement:

One of the authors (JMC) is supported by NIGMS of the National Institutes of Health under award number T32GM007347. The content in this report is solely the responsibility of the authors and does not necessarily represent the official views of the National Institutes of Health.

## References:

1. Dua A, Patel B, Kragh JF, Holcomb JB, Fox CJ. Long-term follow-up and amputation-free survival in 497 casualties with combat-related vascular injuries and damage-control resuscitation. *J Trauma Acute Care Surg.* 2012;73(6):1517–1524. [PubMed: 23188245]
2. Stansbury LG, Lalliss SJ, Branstetter JG, Bagg MR, Holcomb JB. Amputations in U.S. military personnel in the current conflicts in Afghanistan and Iraq. *J Orthop Trauma.* 2008;22(1):43–46. [PubMed: 18176164]
3. Boyer RB, Sexton KW, Rodriguez-Feo CL, et al. Adjuvant neurotrophic factors in peripheral nerve repair with chondroitin sulfate proteoglycan-reduced acellular nerve allografts. *J Surg Res.* 2015;193(2):969–977. [PubMed: 25438961]
4. Gaudet AD, Popovich PG, Ramer MS. Wallerian degeneration: gaining perspective on inflammatory events after peripheral nerve injury. *J Neuroinflammation.* 2011;8:110. [PubMed: 21878126]
5. Barton MJ, John JS, Clarke M, Wright A, Ekberg J. The Glia Response after Peripheral Nerve Injury: A Comparison between Schwann Cells and Olfactory Ensheathing Cells and Their Uses for Neural Regenerative Therapies. *Int J Mol Sci.* 2017;18(2).
6. Boyd JG, Gordon T. Neurotrophic factors and their receptors in axonal regeneration and functional recovery after peripheral nerve injury. *Mol Neurobiol.* 2003;27(3):277–324. [PubMed: 12845152]
7. Gordon T, Tyreman N, Raji MA. The basis for diminished functional recovery after delayed peripheral nerve repair. *J Neurosci.* 2011;31(14):5325–5334. [PubMed: 21471367]

8. Gordon T, Sulaiman O, Boyd JG. Experimental strategies to promote functional recovery after peripheral nerve injuries. *J Peripher Nerv Syst.* 2003;8(4):236–250. [PubMed: 14641648]
9. Sexton KW, Pollins AC, Cardwell NL, et al. Hydrophilic polymers enhance early functional outcomes after nerve autografting. *J Surg Res.* 2012;177(2):392–400. [PubMed: 22521220]
10. Bamba R, Waitayawinyu T, Nookala R, et al. A novel therapy to promote axonal fusion in human digital nerves. *J Trauma Acute Care Surg.* 2016;81(5 Suppl 2 Proceedings of the 2015 Military Health System Research Symposium):S177–S183. [PubMed: 27768666]
11. Lundborg G Alternatives to autologous nerve grafts. *Handchir Mikrochir Plast Chir.* 2004;36(1):1–7. [PubMed: 15083383]
12. Arslantunali D, Dursun T, Yucel D, Hasirci N, Hasirci V. Peripheral nerve conduits: technology update. *Med Devices (Auckl).* 2014;7:405–424. [PubMed: 25489251]
13. Ansselin AD, Davey DF. The regeneration of axons through normal and reversed peripheral nerve grafts. *Restor Neurol Neurosci.* 1993;5(3):225–240. [PubMed: 21551905]
14. Jeon T, Vutescu ES, Saltzman EB, et al. Evaluation of two collagen conduits and autograft in rabbit sciatic nerve regeneration with quantitative magnetic resonance DTI, electrophysiology, and histology. *Eur Radiol Exp.* 2018;2:19. [PubMed: 30148252]
15. Khalil C, Budzik JF, Kermarrec E, Balbi V, Le Thuc V, Cotten A. Tractography of peripheral nerves and skeletal muscles. *Eur J Radiol.* 2010;76(3):391–397. [PubMed: 20392583]
16. Lehmann HC, Zhang J, Mori S, Sheikh KA. Diffusion tensor imaging to assess axonal regeneration in peripheral nerves. *Exp Neurol.* 2010;223(1):238–244. [PubMed: 19879260]
17. Takagi T, Nakamura M, Yamada M, et al. Visualization of peripheral nerve degeneration and regeneration: monitoring with diffusion tensor tractography. *Neuroimage.* 2009;44(3):884–892. [PubMed: 18948210]
18. Noble J, Munro CA, Prasad VS, Midha R. Analysis of upper and lower extremity peripheral nerve injuries in a population of patients with multiple injuries. *J Trauma.* 1998;45(1):116–122. [PubMed: 9680023]
19. Leemans A. ExploreDTI: a graphical toolbox for processing, analyzing and visualizing diffusion MR data; Proceedings of the 17th annual Meeting of international Society for Magnetic Resonance in Medicine; Honolulu, Hawaii. Curran Associates Inc; 2009.
20. Li X, Chen J, Hong G, et al. In vivo DTI longitudinal measurements of acute sciatic nerve traction injury and the association with pathological and functional changes. *Eur J Radiol.* 2013;82(11):e707–714. [PubMed: 23954015]
21. Campbell WW. Evaluation and management of peripheral nerve injury. *Clin Neurophysiol.* 2008;119(9):1951–1965. [PubMed: 18482862]
22. Brushart TM. Preferential reinnervation of motor nerves by regenerating motor axons. *J Neurosci.* 1988;8(3):1026–1031. [PubMed: 3346713]
23. Madison RD, Archibald SJ, Brushart TM. Reinnervation accuracy of the rat femoral nerve by motor and sensory neurons. *J Neurosci.* 1996;16(18):5698–5703. [PubMed: 8795625]
24. Brushart TM. Preferential motor reinnervation: a sequential double-labeling study. *Restor Neurol Neurosci.* 1990;1(3):281–287. [PubMed: 21551568]
25. Nichols CM, Brenner MJ, Fox IK, et al. Effects of motor versus sensory nerve grafts on peripheral nerve regeneration. *Exp Neurol.* 2004;190(2):347–355. [PubMed: 15530874]
26. Sun SW, Neil JJ, Liang HF, et al. Formalin fixation alters water diffusion coefficient magnitude but not anisotropy in infarcted brain. *Magn Reson Med.* 2005;53(6):1447–1451. [PubMed: 15906292]

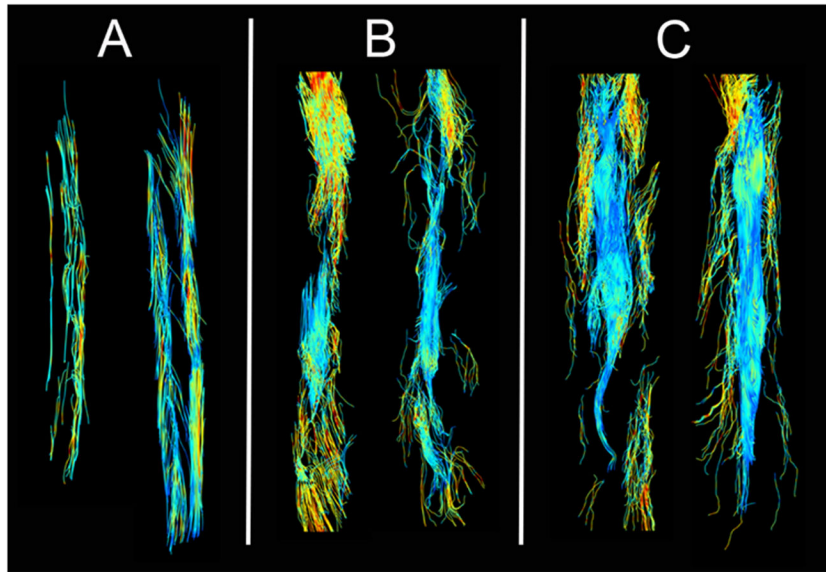


**Figure 1. Representative DTT images of Ex-Vivo Nerves**  
Normal (A), 6-week reverse autograft (B), 11-week reverse autograft (C).

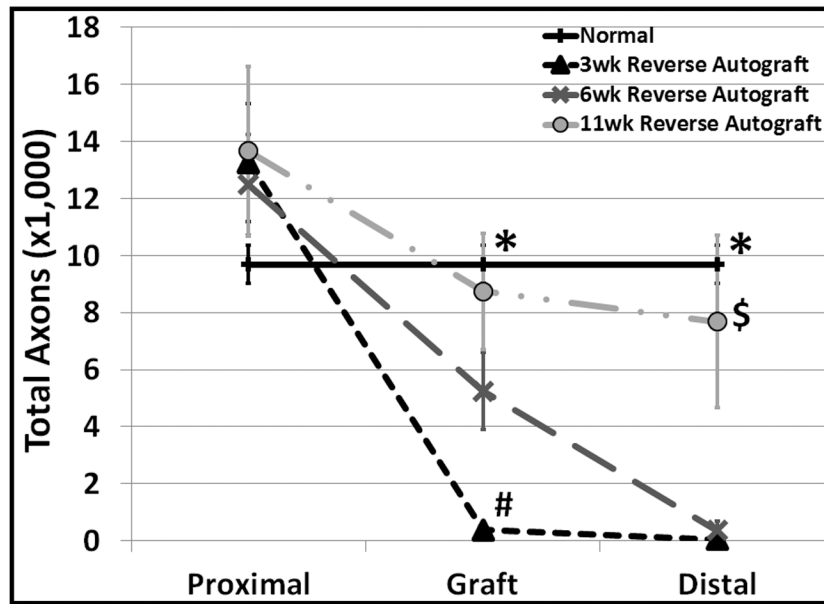


**Figure 2. Total Mean Axon Counts at 3 Different Distances along the Nerve Repair Site**  
 Total Axon Counts. Normal (n=9), 3 week (n=7), 6 week (n=5), and 11 week (n=6) reverse autografts. \*p < 0.05 Normal vs. 3 week and normal vs. 6wk; # p < 0.05 3 week vs. 6 week and 3 week vs. 11 week; \$ p < 0.05 11 week vs. 3 week and 11 week vs. 6 week.

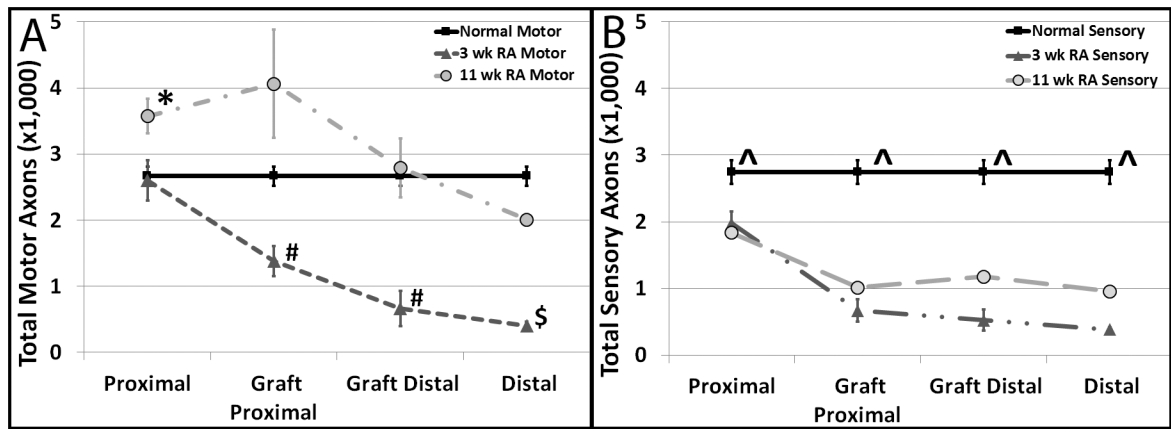


**Figure 3. Total Mean Motor (A) and Sensory (B) Axon Counts at 4 Different Distances Along the Nerve Repair Site**

A) Motor Axons. Normal (n=10), 3 week (n=5), and 11 week (n=3, except distal (n=2)) reverse autografts. \*p < 0.05 11 week vs Normal and 11 week vs. 3 week; # p < 0.05 3 week vs. normal and 3 week vs. 11 week; \$ p < 0.05 3 week vs. normal. B) Sensory Axons. Normal (n=9), 3 week (n=5), and 11 week (n=2) reverse autografts. ^p < 0.05 normal vs. 3 week reverse autograft.